

A Simple Spectral Failure Mode for Graph Convolutional Networks

Carey E. Priebe, Cencheng Shen, Ningyuan (Teresa) Huang, Tianyi Chen

Abstract—We present a simple generative model in which spectral graph embedding for subsequent inference succeeds whereas unsupervised graph convolutional networks (GCN) fail. The geometrical insight is that the GCN is unable to look beyond the first non-informative spectral dimension.

Index Terms—Graph embedding, Vertex classification, Convolutional neural net

1 INTRODUCTION

THE classical statistical formulation of the classification problem consists of

$$(X, Y), (X_1, Y_1), \dots, (X_m, Y_m) \stackrel{iid}{\sim} F_{XY}$$

where $\mathcal{T}_m = \{(X_i, Y_i)\}_{i \in \{1, \dots, m\}}$ is the training data and (X, Y) represents the to-be-classified test observation X with true-but-unobserved class label Y . We consider the simple setting in which X is a feature vector in finite-dimensional Euclidean space and Y is a class label in $\{0, 1\}$. For $y \in \{0, 1\}$, let $F_y = F_{X|Y=y}$ be the class-conditional distributions and $\pi_y = P[Y = y]$ be the class-conditional prior probabilities. The marginal distribution of X is given by $F_X = \pi_0 F_0 + \pi_1 F_1$. We assume that X has a density, and denote by f_X and f_y the marginal and class-conditional densities. We denote the Bayes optimal classifier $g^*(\cdot) = \arg \max_y \pi_y f_y(\cdot)$ and its associated Bayes optimal probability of misclassification by $L^* = P[g^*(X) \neq Y]$.

The goal is to learn a classification rule $g_m = g(\cdot; \mathcal{T}_m)$ mapping feature vectors to class labels such that the probability of misclassification $L(g_m) = P[g(X; \mathcal{T}_m) \neq Y | \mathcal{T}_m]$ is small (see [1], page 2). In this paper we shall assume that the class of rules under consideration \mathcal{C} is all linear classifiers and that $g^* \in \mathcal{C}$. We will evaluate performance via the expectation (taken over the training data) of probability of misclassification, $E[L(g_m)]$. In this setting, choosing $g_m \in \mathcal{C}$ via empirical risk minimization (ERM) yields $E[L(g_m)] \rightarrow L^*$ as $m \rightarrow \infty$ (see [1], Theorem 4.5).

- Carey E. Priebe is with the Department of Applied Mathematics and Statistics (AMS), the Center for Imaging Science (CIS), and the Mathematical Institute for Data Science (MINDS), Johns Hopkins University. E-mail: cep@jhu.edu
- Cencheng Shen is with the Department of Applied Economics and Statistics, University of Delaware. E-mail: shenc@udel.edu
- Ningyuan (Teresa) Huang and Tianyi Chen are with the Department of Applied Mathematics and Statistics, Johns Hopkins University. E-mail: nhuang19@jhu.edu, tchen94@jhu.edu

This work was supported in part by the Defense Advanced Research Projects Agency under the D3M program administered through contract FA8750-17-2-0112, NSF HDR TRIPODS award #1934979, and by funding from Microsoft Research. The authors thank Wade Shen for providing the motivation for this investigation.

2 A LATENT POSITION GRAPH

The generative model of interest in this paper involves

$$(X_1, Y_1), \dots, (X_n, Y_n) \stackrel{iid}{\sim} F_{XY}$$

with univariate marginal distribution F_X satisfying $P[X_i X_j \in [0, 1]] = 1$. As such, we may assume without loss of generality that the marginal density f_X is supported on the unit interval $[0, 1]$.

However, rather than observing the X_i 's, we observe a latent position graph $G = (V, E)$ on n vertices with (binary, symmetric, hollow) adjacency matrix A . In particular, we consider $A_{ij} \stackrel{iid}{\sim} \text{Bernoulli}(X_i X_j)$ for $i < j$. This is the so-called random dot product graph (RDPG); see [2] for a recent survey.

We observe the $n \times n$ matrix A , but we only observe the class labels Y_i for $m < n$ of the vertices. The task is to classify the remaining $n - m$ vertices. This is a simple case of the problem studied in [3].

3 GRAPH EMBEDDING

Given the $n \times n$ matrix A and Y_1, \dots, Y_m , we approach the vertex classification task via unsupervised graph embedding followed by subsequent linear classification. Specifically, we consider embedding, denoted $h : A_{n \times n} \rightarrow (\mathbb{R}^d)^n$, via adjacency spectral embedding (ASE: the scaled leading eigenvectors $U_d |\Sigma_d|^{1/2}$ of A) [4] and graph convolution networks (GCN) [5], [6]. (Other graph embedding methods, not germane to our investigation but popular nonetheless, include Laplacian spectral embedding [7], node2vec [8], etc.) In any case, $h(A) = \{\hat{X}_1, \dots, \hat{X}_n\}$, a classifier $\hat{g}_{m,n}$ is trained on $\hat{\mathcal{T}}_{m,n} = \{(\hat{X}_i, Y_i)\}_{i \in \{1, \dots, m\}}$, and for $i > m$ our classification is given by $\hat{g}_{m,n}(\hat{X}_i)$. Performance is measured via $E[L(\hat{g}_{m,n})]$.

Note that $E[L(g_m)]$ is the target performance – the performance we would achieve if we observed the latent positions themselves. We cannot hope to do better, as our $(X_i X_j)$'s are corrupted through the Bernoulli noise channel into A_{ij} , via an argument reminiscent of the data processing lemma. RDPG theory for ASE into dimension $d = \text{rank}(E[A]) = 1$ — specifically the $2 \rightarrow \infty$

norm convergence result presented in [9] — implies that $E[L(\hat{g}_{m,n})] \rightarrow E[L(g_m)]$ as $n \rightarrow \infty$. However, to the best of our knowledge, there is no such theoretical guarantee for GCN despite its empirical success in real-world data applications.

4 THE srt TRANSFORMATION

Now we consider a transformation $Z = srt(X)$ taking f_X on $[0, 1]$ to f_Z on line segment $S \subset \mathbb{R}^2$. Thus $Z_i = [Z_{i1}, Z_{i2}]^\top = srt(X_i)$ for $i \in \{1, \dots, n\}$. We require that the inner product constraint $P[Z_i^\top Z_j \in [0, 1]] = 1$ be preserved. As such, we may assume without loss of generality that the marginal density f_Z is supported on $S \subset \mathbb{R}_+^2 \cap B(0, 1)$.

To be precise, we scale ($s \in \mathbb{R}_+$), rotate about the origin (angle $r \in [0, 2\pi)$), and translate ($t \in \mathbb{R}^2$) via

$$Z = srt(X) = \begin{bmatrix} \cos(r) & -\sin(r) \\ \sin(r) & \cos(r) \end{bmatrix} \begin{bmatrix} sX \\ 0 \end{bmatrix} + t.$$

Properly constrained — to preserve the inner product constraint, the range of (s, r, t) is a proper subset of $\mathbb{R}_+ \times [0, 2\pi) \times \mathbb{R}^2$ — the function srt takes the interval $[0, 1]$ to segment $S \subset \mathbb{R}_+^2 \cap B(0, 1)$, in which case an RDPG G_{srt} is available via $Bernoulli(Z_i^\top Z_j)$.

Note that $E[A_{srt}]$ is positive semidefinite and, except for very special values for (s, r, t) for which S is on a ray from the origin, we have $\text{rank}(E[A_{srt}]) = 2$. Both L^* and $E[L(g_m)]$ remain unchanged under the srt transformation.

5 FAILURE GEOMETRY

Figure 1 illustrates the failure mode for GCN. The marginal f_Z is supported on the line segment $S \subset \mathbb{R}_+^2 \cap B(0, 1)$. There are two angles of interest: θ_\perp is the angle between \mathbb{R}_+ and the ray from the origin perpendicular to S ; θ_E is the angle between \mathbb{R}_+ and the ray from the origin to $E[Z]$. When $\theta_E = \theta_\perp$, GCN fails. In this case, the first eigenvector of $E[A_{srt}]$ is orthogonal to S and the first dimension of the ASE embedding of A_{srt} captures (essentially) no signal. While $E[L(\hat{g}_{m,n})]$ can be inflated for finite n , we still have $E[L(\hat{g}_{m,n})] \rightarrow E[L(g_m)]$ as $n \rightarrow \infty$ so long as ASE is now into dimension $d = 2$. However, neither GCN nor ASE into dimension $d = 1$ can find the signal when the first eigenvector of A_{srt} is (approximately) orthogonal to S .

6 FAILURE SIMULATION

As in Figure 1, let F_{XY} be given by $f_0 = \text{Beta}(10, 3)$, $f_1 = \text{Beta}(4, 3)$, and $\pi_0 = \pi_1 = 1/2$. Figure 2 shows one example ASE for this case, with $(s, r, t) = (1.1, 53\pi/32, [0.13, 0.97]^\top)$, for which $\theta_\perp = 5\pi/32$ and $\theta_E = 3\pi/16$ and hence $|\theta_E - \theta_\perp| = \pi/32$. For this case, $L^* \approx 0.25$ and $E[L(g_{100})] \approx 0.26$; Monte Carlo simulation with $m = 100$ and $n = 1000$ yields $E[L(\hat{g}_{100,1000})] \approx 0.28$ for ASE with $d = 2$, 0.36 for ASE with $d = 1$, and 0.40 for unsupervised GCN produced by an unsupervised two-layer GCN model with hidden size $d = 2$, learning rate 0.01 and no weight decay (see Section 7 for GCN details). Note that the selected embedding dimension for ASE — the number of “large” eigenvalues of A — is clearly $d = \text{rank}(E[A_{srt}]) = 2$.

More generally, we consider $(s, r, t) = (1.1, 53\pi/32, t)$. As t ranges linearly from $[0.25, 0.97]^\top$ to $[0.02, 0.97]^\top$,

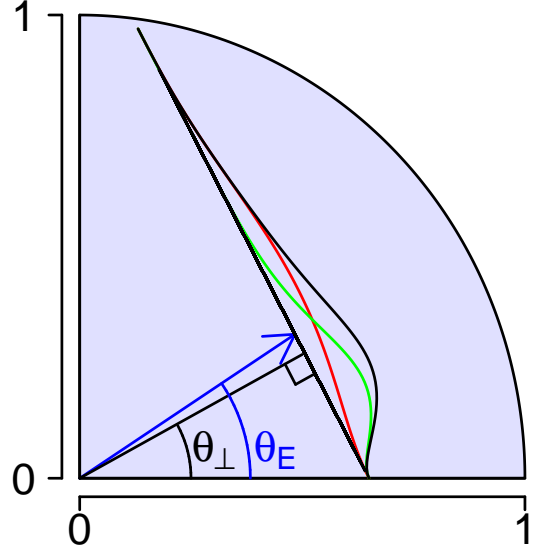


Fig. 1. Geometry for the canonical case where ASE succeeds but GCN fails. The key is $|\theta_E - \theta_\perp|$.

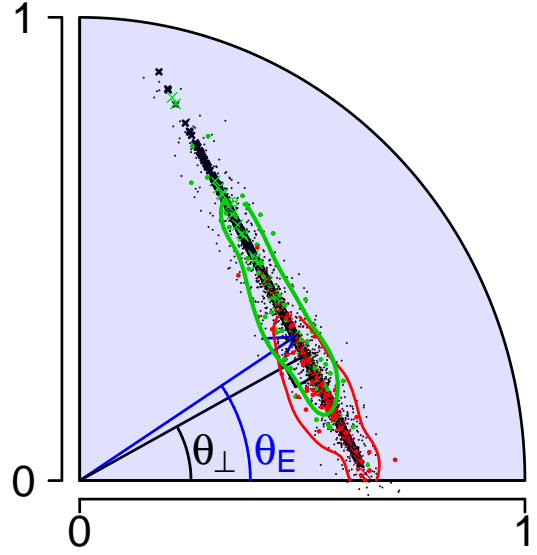


Fig. 2. Example ASE for the geometry depicted in Figure 1 with $n = 1000$, illustrating the dearth of signal captured by the first eigenvector of A_{srt} when $\theta_E \approx \theta_\perp$. For this case, indicated by the vertical line at $|\theta_E - \theta_\perp| = \pi/32$ in Figure 3, both ASE into dimension $d = 1$ and unsupervised two-layer GCN perform poorly while ASE into two dimensions performs nearly optimally.

$|\theta_E - \theta_\perp|$ ranges from 0 to $\pi/14$. Figure 3 shows Monte Carlo simulation results for this case, with $m = 100$ and $n = 1000$. The classifier $\hat{g}_{m,n}$ using ASE into two dimensions works well across the entire range with slight degradation for $|\theta_E - \theta_\perp|$ small, while both unsupervised GCN and ASE into one dimension yield classifiers which degrade drastically for $|\theta_E - \theta_\perp| \approx 0$. (Figures 1 and 2 show $|\theta_E - \theta_\perp| = \pi/32$ – the vertical line in Figure 3.)

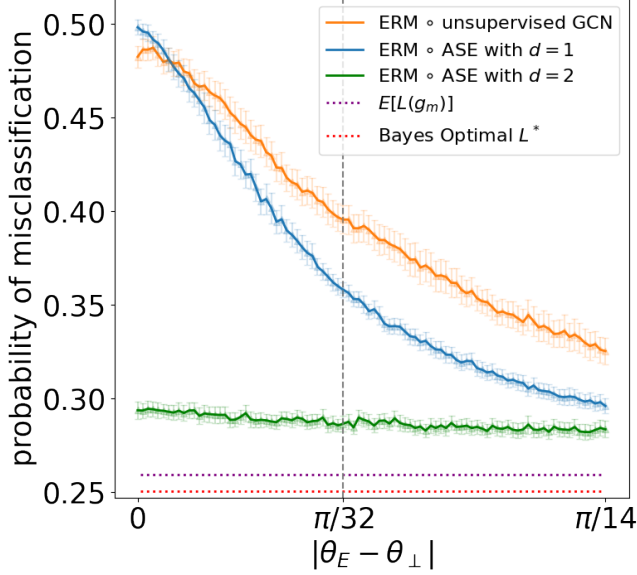


Fig. 3. Performance for the canonical case where ASE succeeds but two-layer unsupervised linear GCN fails. For $\theta_E \approx \theta_\perp$, the first eigenvector of A_{src} captures (essentially) no signal. ERM in the legend stands for empirical risk minimization classifier.

7 GRAPH CONVOLUTIONAL NETWORKS

The unsupervised GCN results presented in Figure 3 are obtained without hyper-parameter search, using hidden size $d = 2$, learning rate 0.01 and weight decay 0. In this section we provide details for the unsupervised GCN considered, a semisupervised version which performs more like ASE, and results for both including hyperparameter search.

We consider a two-layer GCN model [5] designed as

$$GCN(\mathbf{X}, A) = \tilde{A} \text{ReLU}(\tilde{A} \mathbf{X} W_0) W_1 \quad (1)$$

where \mathbf{X} is the data matrix with X_i in its rows and $\tilde{A} = D^{-1/2} A D^{-1/2}$ is the symmetrically normalized adjacency matrix with D being the node degree matrix. Note that in the GCN model, the adjacency matrix A has self-edges. In our setting without any additional node features, the input \mathbf{X} is a one-hot embedding matrix (i.e, the identity matrix in \mathbb{R}^n).

One may derive **linear** GCN by replacing ReLU nonlinearity with the identity function. Hereafter we use linear GCN to simplify the analysis, as our set-up in Section 6 is linear.

7.1 Unsupervised GCN

Unsupervised GCN (Variational Graph Auto-Encoder [6]) estimates the latent graph embedding matrix $\hat{\mathbf{X}}$ using a

variational Auto-Encoder architecture without seeing any labels. The variational inference model of $\hat{\mathbf{X}}$ is given by

$$q(\hat{\mathbf{X}}|\mathbf{X}, A) = \prod_{i=1}^n q(\hat{X}_i|\mathbf{X}, A)$$

with $q(\hat{X}_i|\mathbf{X}, A) = \mathcal{N}(\hat{X}_i|\boldsymbol{\mu}_i, \text{diag}(\boldsymbol{\sigma}_i^2))$. In our linear GCN setting, the parameters of the inference model $\boldsymbol{\mu}, \boldsymbol{\sigma}$ (the matrix of mean vectors $\boldsymbol{\mu}_i$ and variance vectors $\boldsymbol{\sigma}_i$ respectively) are estimated as

$$\boldsymbol{\mu} = GCN_{\boldsymbol{\mu}}(\mathbf{X}, A) = \tilde{A} \tilde{A} W_0 W_1^{\boldsymbol{\mu}} \quad (2)$$

$$\log \boldsymbol{\sigma} = GCN_{\boldsymbol{\sigma}}(\mathbf{X}, A) = \tilde{A} \tilde{A} W_0 W_1^{\boldsymbol{\sigma}} \quad (3)$$

where $GCN_{\boldsymbol{\mu}}$ and $GCN_{\boldsymbol{\sigma}}$ share the first layer weights W_0 and learn the second layer weights $W_1^{\boldsymbol{\mu}}, W_1^{\boldsymbol{\sigma}}$ independently.

Unsupervised GCN is trained by minimizing the variational lower bound \mathcal{L} with respect to $W_0, W_1^{\boldsymbol{\mu}}, W_1^{\boldsymbol{\sigma}}$:

$$\mathcal{L}_{unsup} = \mathbb{E}_{q(\hat{\mathbf{X}}|\mathbf{X}, A)} [\log p(A|\hat{\mathbf{X}})] - KL[q(\hat{\mathbf{X}}|\mathbf{X}, A) || p(\hat{\mathbf{X}})] \quad (4)$$

where the $KL[q(\cdot)||p(\cdot)]$ term represents the Kullback-Leibler divergence between $q(\cdot)$ and $p(\cdot)$. We assume a Gaussian prior $p(\hat{\mathbf{X}}) = \prod_i \mathcal{N}(\hat{X}_i|0, \mathbf{I})$. In the training stage, the embedding is estimated using the reparameterization trick [10] as $\hat{\mathbf{X}} = \boldsymbol{\mu} + \epsilon \exp \log \boldsymbol{\sigma}$. The subsequent inference of the embedding is made by $\hat{\mathbf{X}} = \boldsymbol{\mu}$.

7.2 Semisupervised GCN

One may approach the vertex classification task considered herein with an end-to-end learning framework that outputs the class labels Y from the input A directly. The semisupervised GCN produces the class probabilities as

$$P = \text{softmax}(GCN(\mathbf{X}, A)). \quad (5)$$

We train with m labels and test on the remaining $n - m$ labels as described in Section 2, using cross-entropy loss

$$\mathcal{L}_{semisup} = - \sum_{i=1}^m \sum_{j=1}^c Y_{ij} \log P_{ij} \quad (6)$$

where c represents the number of classes ($c = 2$ in our binary case).

7.3 Experiment

We further demonstrate that even with hyper-parameter search, unsupervised GCN still fails the aforementioned simulation while semisupervised GCN does not outperform ASE. We use the following parameter grid for both GCN models:

- Hidden size (d): [2, 4]
- Learning rate: [0.01, 0.001]

Unsupervised GCN is trained on all n nodes while semisupervised GCN is trained on m nodes with additional labels Y . Both GCN models are trained for a maximum of 500 epochs with early stopping at a patience of 100 epochs. For semisupervised GCN, we also experiment with further splitting m nodes into 80% training set and 20% validation set, and use early stopping based on validation (see yellow crosses in Figure 4).

We repeat the hyper-parameter search on 10 different weight initializations. Then the setting with the best average training accuracy (validation accuracy for cross-validation semisupervised GCN) is chosen as our estimate of the optimal hyper-parameter ($\hat{\theta}_{GCN}^*$). The test error is calculated by fitting the best check-point model of $\hat{\theta}_{GCN}^*$ on the $n - m$ labels. This procedure is applied on every single Monte Carlo replicate, allowing each observation to have its own optimized $\hat{\theta}_{GCN}^*$.

The results are presented in Figure 4: unsupervised GCN still fails even after optimizing for hyper-parameters (see orange stars), while semisupervised GCN performs much better but still slightly worse than ASE into two dimensions (see yellow stars for no validation case, and yellow crosses for cross-validation case).

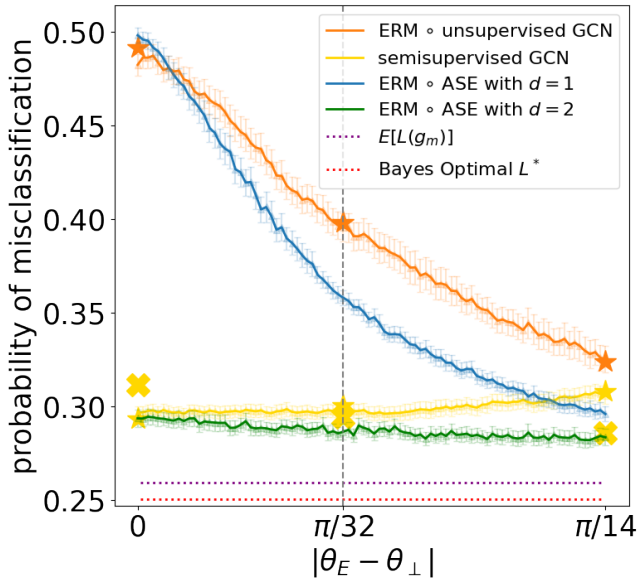


Fig. 4. In the setting of Section 6 and Figure 3, when optimizing GCN hyperparameters, unsupervised GCN still fails while semisupervised GCN performance approaches that of ASE into two dimensions. The orange and yellow curves for both GCN models are obtained without hyper-parameter search, while the orange and yellow stars (crosses for cross-validation semisupervised GCN) represent the best results after hyper-parameter search. Notice that although semi-supervised GCN doesn't fail, it entails a trade-off between underfitting when the signal is sparse and overfitting when the signal is abundant, and thus requires careful experimental design.

8 CONCLUSION

The purpose of this short note is to illustrate a simple spectral failure mode for Graph Convolutional Networks in the context of the classical statistical formulation of the classification problem. Generalization of the phenomenon to more realistic and applicable settings (multivariate X , more complex model/discriminant boundary, etc.) is straightforward, but the fundamental idea is here presented in its fullest simplicity.

Note that the stochastic block model (SBM) is a special (point masses) case of our RDPG/*srt* model, and from [11] Lemma 3 we see that our model encompasses the mixed membership SBM (MMSBM), as well as the degree

corrected SBM (DCSBM). Furthermore, our story can easily be extended to the case of $\text{rank}(E[A]) > 2$ and to weighted and/or directed graphs, as well as to the indefinite case. Note also that it is easy to choose ASE embedding dimension $\hat{d} = d$ – see e.g. universal singular value thresholding [12].

The theory for failure of ASE into $d = 1$ when $\theta_E = \theta_\perp$ is straightforward; for unsupervised GCN, the theory for failure in the case of a regular graph is available (see [13], [14] where GCN fails to distinguish non-isomorphic regular graphs, and [15] for a comprehensive survey of the expressive power of graph neural networks), and our failure mode $\theta_E = \theta_\perp$ implies constant expected degree. The superiority of ASE into $d = 2$ is equally straightforward: for an RDPG, ASE provides the correct embedding representation (albeit with a wasted dimension when $\theta_E = \theta_\perp$).

While the RDPG generative model has inherent orthogonal nonidentifiability, the classification task considered herein is invariant to this nonidentifiability. (Note that the embedding in Figure 2 is presented after orthogonal Procrustes transformation, for illustrative purposes.)

The use case considered herein – a large number of vertices n but a small number of labeled vertices m – is relevant in many applications. A general comparison of inherently unsupervised spectral graph embedding followed by subsequent classification versus state-of-the-art semisupervised GCN is beyond the scope of this paper. However, as noted above, when a simple spectral embedding provides a good representation and the training sample size is small then it is likely that the added GCN embedding complexity will prove to be a hindrance in terms of the bias-variance trade-off. As noted in [1]: “Simple rules survive.”

REFERENCES

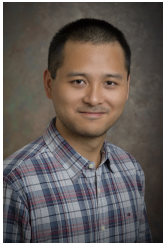
- [1] L. Devroye, L. Györfi, and G. Lugosi, *A Probabilistic Theory of Pattern Recognition*, ser. Stochastic Modelling and Applied Probability. Springer New York, 1997.
- [2] A. Athreya, D. E. Fishkind, M. Tang, C. E. Priebe, Y. Park, J. T. Vogelstein, K. Levin, V. Lyzinski, Y. Qin, and D. L. Sussman, “Statistical inference on random dot product graphs: a survey,” *Journal of Machine Learning Research*, vol. 18, no. 226, pp. 1–92, 2018.
- [3] M. Tang, D. L. Sussman, and C. E. Priebe, “Universally consistent vertex classification for latent positions graphs,” *Annals of Statistics*, vol. 41, no. 3, pp. 1406–1430, 2013.
- [4] D. L. Sussman, M. Tang, D. E. Fishkind, and C. E. Priebe, “A consistent adjacency spectral embedding for stochastic blockmodel graphs,” *Journal of the American Statistical Association*, vol. 107, no. 499, pp. 1119–1128, 2012.
- [5] T. N. Kipf and M. Welling, “Semi-supervised classification with graph convolutional networks,” *arXiv preprint arXiv:1609.02907*, 2016.
- [6] —, “Variational graph auto-encoders,” *arXiv preprint arXiv:1611.07308*, 2016.
- [7] U. Von Luxburg, “A tutorial on spectral clustering,” *Statistics and Computing*, vol. 17, no. 4, pp. 395–416, 2007.
- [8] A. Grover and J. Leskovec, “node2vec: Scalable feature learning for networks,” in *Proceedings of the 22nd ACM SIGKDD international conference on Knowledge discovery and data mining*, 2016, pp. 855–864.
- [9] J. Cape, M. Tang, and C. E. Priebe, “The two-to-infinity norm and singular subspace geometry with applications to high-dimensional statistics,” *Annals of Statistics*, vol. 47, no. 5, pp. 2405–2439, 10 2019.
- [10] D. P. Kingma and M. Welling, “Auto-encoding variational bayes,” *arXiv preprint arXiv:1312.6114*, 2013.
- [11] P. Rubin-Delanchy, C. E. Priebe, and M. Tang, “Consistency of adjacency spectral embedding for the mixed membership stochastic blockmodel,” *arXiv preprint arXiv:1705.04518*, 2017.

- [12] S. Chatterjee, "Matrix estimation by universal singular value thresholding," *The Annals of Statistics*, vol. 43, no. 1, p. 177–214, 2015.
- [13] K. Xu, W. Hu, J. Leskovec, and S. Jegelka, "How powerful are graph neural networks?" in *Proc. ICLR*, 2019, pp. 1–17.
- [14] Z. Chen, L. Chen, S. Villar, and J. Bruna, "Can graph neural networks count substructures?" *arXiv preprint arXiv:2002.04025*, 2020.
- [15] R. Sato, "A survey on the expressive power of graph neural networks," *arXiv preprint arXiv:2003.04078*, 2020.

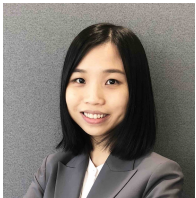


Carey E. Priebe received the BS degree in mathematics from Purdue University in 1984, the MS degree in computer science from San Diego State University in 1988, and the PhD degree in information technology (computational statistics) from George Mason University in 1993. From 1985 to 1994 he worked as a mathematician and scientist in the US Navy research and development laboratory system. Since 1994 he has been a professor in the Department of Applied Mathematics

and Statistics at Johns Hopkins University. His research interests include computational statistics, kernel and mixture estimates, statistical pattern recognition, model selection, and statistical inference for high-dimensional and graph data. He is a Senior Member of the IEEE, an Elected Member of the International Statistical Institute, a Fellow of the Institute of Mathematical Statistics, and a Fellow of the American Statistical Association.



Cencheng Shen received the BS degree in Quantitative Finance from National University of Singapore in 2010, and the PhD degree in Applied Mathematics and Statistics from Johns Hopkins University in 2015. He is assistant professor in the Department of Applied Economics and Statistics at University of Delaware. His research interests include testing independence, correlation measures, dimension reduction, and statistical inference for high-dimensional and graph data.



Ningyuan (Teresa) Huang received the BS degree in Statistics from the University of Hong Kong, the MS degree in Data Science from New York University, and is currently pursuing her PhD in the Department of Applied Mathematics and Statistics at Johns Hopkins University. She is interested in representation learning, the theory of deep learning, and inter-disciplinary research in data science.



Tianyi Chen received the BS degree in Statistics from Renmin University of China, and is currently pursuing his masters degree in the Department of Applied Mathematics and Statistics at Johns Hopkins University.